

Cosmology with galaxy clusters: An improved multi-wavelength analysis

Gaspard Aymerich

Marian Douspis, Laura Salvati

Institut d'Astrophysique Spatiale

Gabriel Pratt

Astrophysique Interactions Multi-Echelles, CEA

Felipe Andrade-Santos, William Forman, Christine Jones

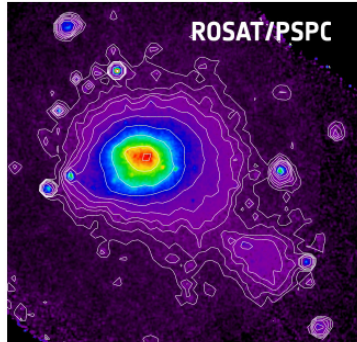
Center for Astrophysics, Harvard

Observing galaxy clusters

How can we observe them ?

Different wavelengths probe different properties of clusters

Combining all wavelengths allow for more precise characterisation of cluster properties

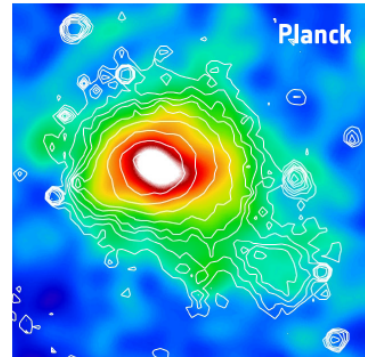


X-ray emission:
Bremsstrahlung

Sensitive to **gas density squared**

High resolution

$$E_X \propto \int_V n_e^2 \Lambda(T) dV$$



mm-wavelength:

Thermal Sunyaev-Zeldovich effect

(inverse Compton scattering)

Sensitive to **gas pressure**

$$F_\nu \propto \int_\Omega (P = n_e T) d\Omega$$



Optical/near IR wavelength:

Stars (small part of total mass)

Gravitational lensing

(total mass, limited precision)

Combining X-ray and SZ

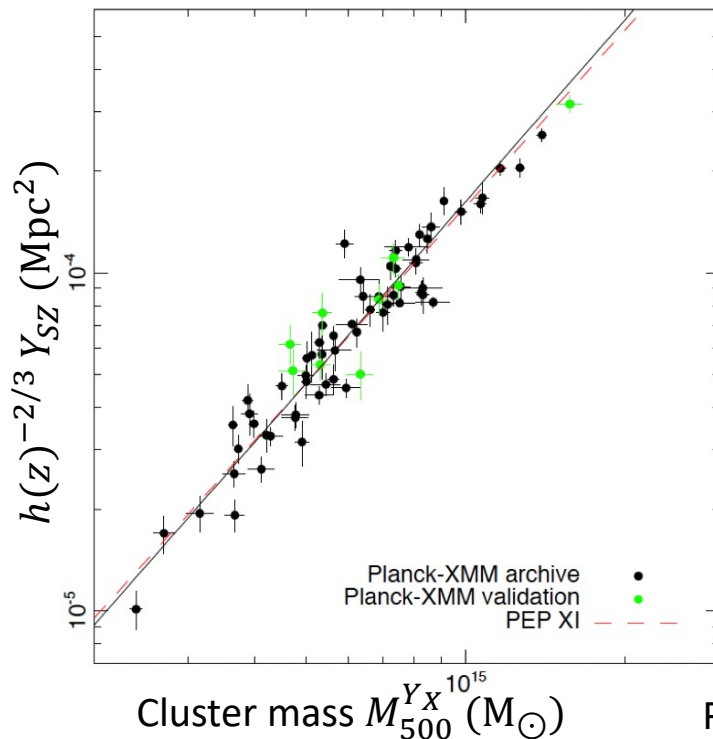
First step: improving on Planck 2015

Planck data provides full sky SZ-survey: great opportunity for cosmological analysis

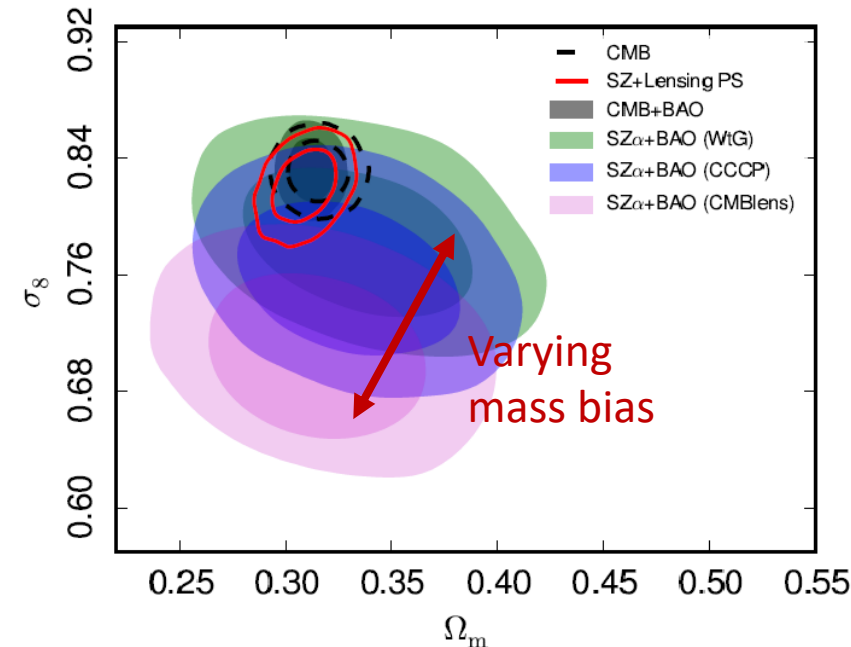
Cluster mass can't be directly inferred from SZ signal

Arnaud et al. 2010 relates X-ray signal from XMM-Newton to mass under hydrostatic equilibrium assumption

Y500-M500 is calibrated on a common XMM/SZ set of 71 clusters: $E^{-2/3}(z) \left[\frac{D_A^2 Y_{500}}{10^{-4} \text{ Mpc}^2} \right] = 10^{-0.19 \pm 0.02} \left(\frac{(1-b) M_{500}}{6 \times 10^{14} M_\odot} \right)^{1.79 \pm 0.08}$



Planck 2013



Planck 2015

Combining X-ray and SZ

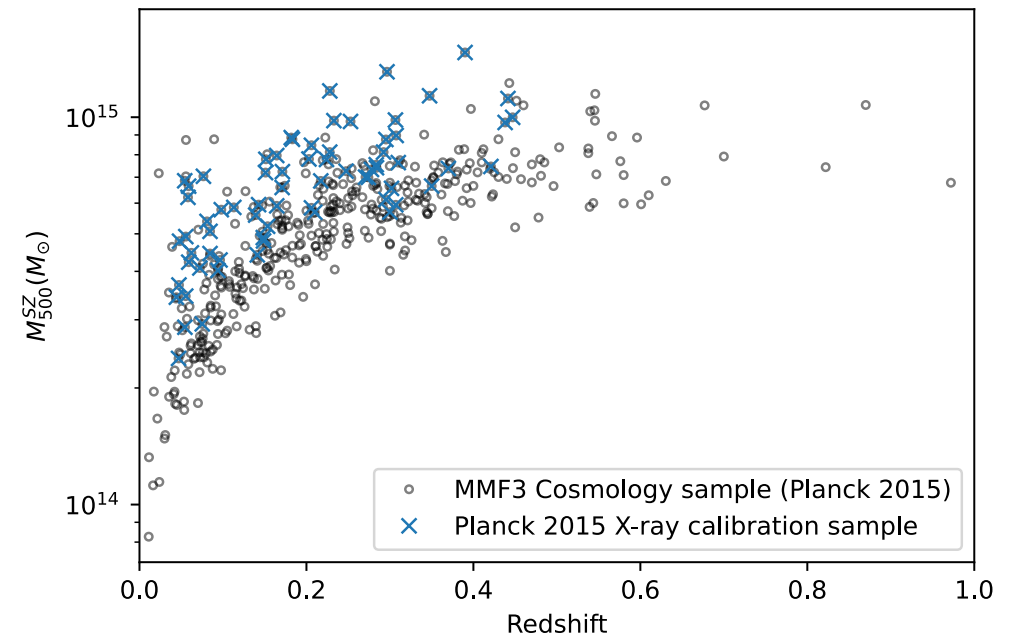
First step: improving on Planck 2015

Planck data provides full sky SZ-survey: great opportunity for cosmological analysis

Cluster mass can't be directly inferred from SZ signal

Arnaud et al. 2010 relates X-ray signal from XMM-Newton to mass under hydrostatic equilibrium assumption

Y500-M500 is calibrated on a common XMM/SZ set of 71 clusters: $E^{-2/3}(z) \left[\frac{D_A^2 Y_{500}}{10^{-4} \text{ Mpc}^2} \right] = 10^{-0.19 \pm 0.02} \left(\frac{(1-b) M_{500}}{6 \times 10^{14} M_\odot} \right)^{1.79 \pm 0.08}$



Combining X-ray and SZ

First step: improving on Planck 2015

Planck data provides full sky SZ-survey: great opportunity for cosmological analysis

Cluster mass can't be directly inferred from SZ signal

Arnaud et al. 2010 relates X-ray signal from XMM-Newton to mass under hydrostatic equilibrium assumption

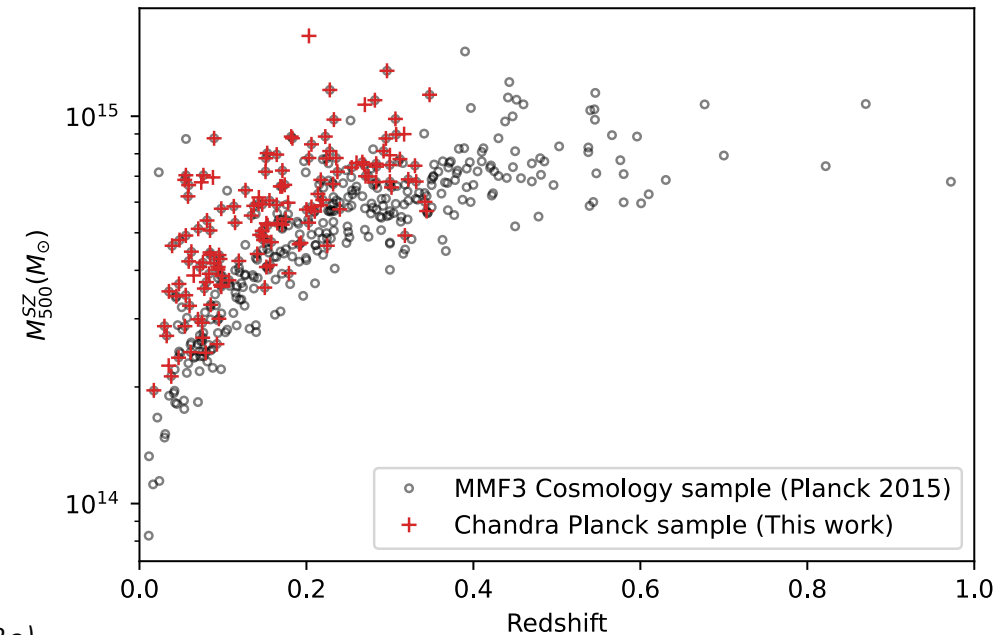
~~Y500-M500 is calibrated on a common XMM/SZ set of 71 clusters:~~

$$E^{-2/3}(z) \left[\frac{D_A^2 Y_{500}}{10^{-4} \text{ Mpc}^2} \right] = 10^{0.19 \pm 0.02} \left(\frac{(1-b) M_{500}}{6 \times 10^{14} M_\odot} \right)^{1.79 \pm 0.08}$$

146 clusters from Planck ESZ sample were observed by Chandra



More clusters
Better low-mass leverage
Similar high-mass leverage
Better low-redshift leverage
Slightly worse high-redshift leverage



Combining X-ray and SZ

First step: improving on Planck 2015

Planck data provides full sky SZ-survey: great opportunity for cosmological analysis

Cluster mass can't be directly inferred from SZ signal

Arnaud et al. 2010 relates X-ray signal from XMM-Newton to mass under hydrostatic equilibrium assumption

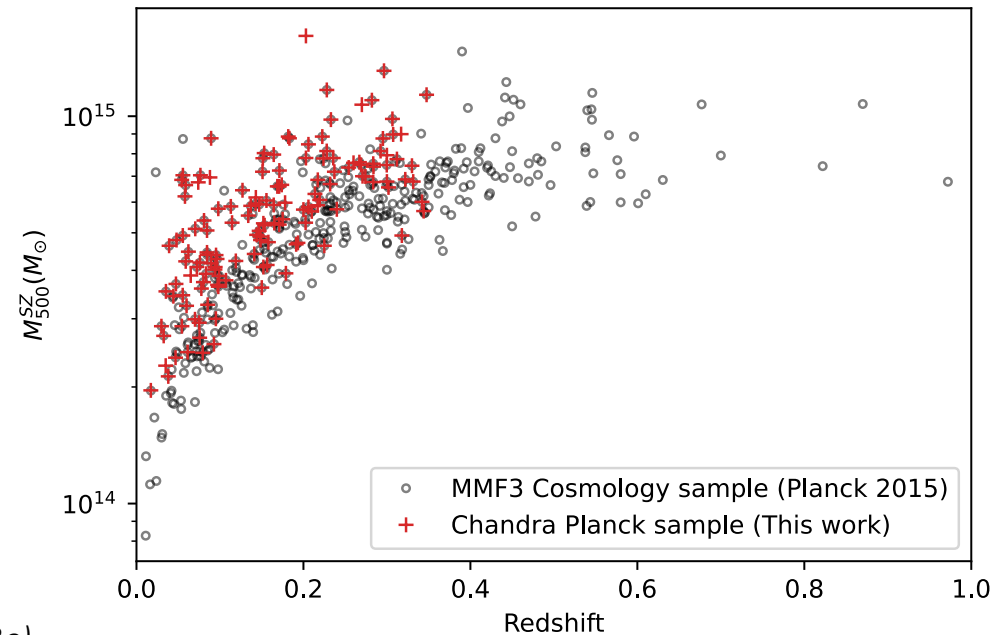
~~Y500-M500 is calibrated on a common XMM/SZ set of 71 clusters:~~

$$E^{-2/3}(z) \left[\frac{D_A^2 Y_{500}}{10^{-4} \text{ Mpc}^2} \right] = 10^{0.19 \pm 0.02} \left(\frac{(1-b) M_{500}}{6 \times 10^{14} M_\odot} \right)^{1.79 \pm 0.08}$$

146 clusters from Planck ESZ sample were observed by Chandra



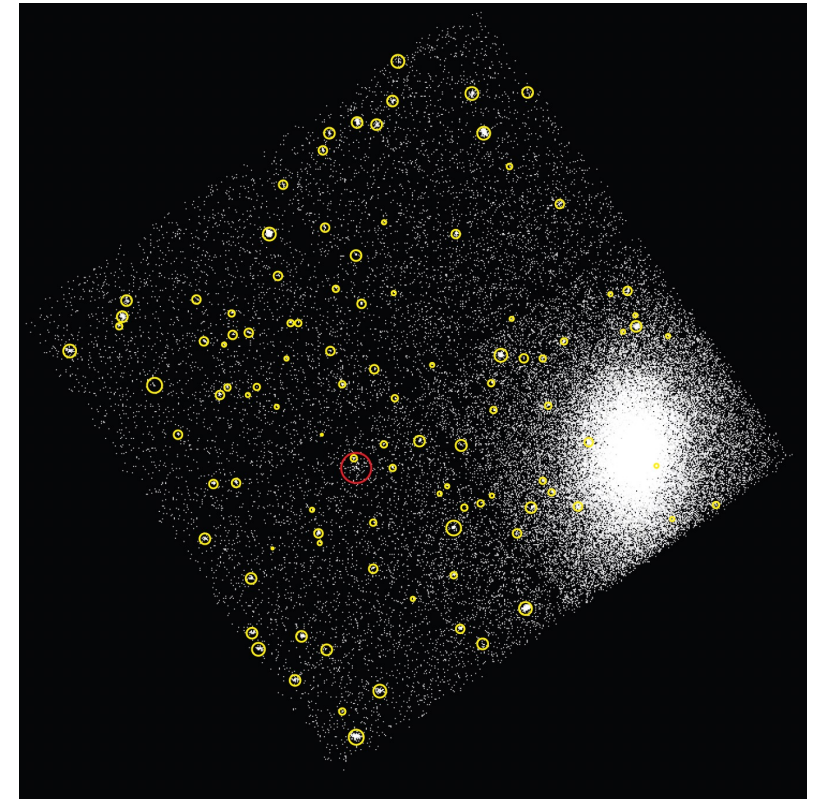
Analyse the data and calibrate a new scaling relation
Constrain cosmological parameters



Analysis of X-ray data

Data processing: from event file to profiles

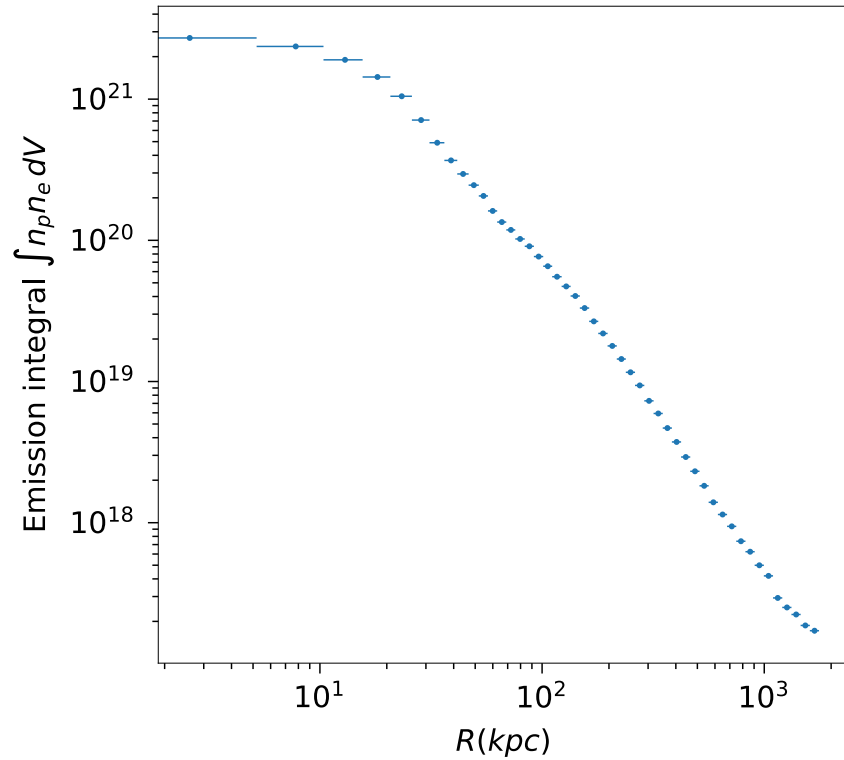
- Charge-transfer inefficiency, mirror contamination, CCD non-uniformity and time dependence of gain are corrected
- Blank sky and readout artifacts are subtracted
- X-ray point sources and extended substructures are masked
- Surface brightness profile is extracted in the 0.7-2keV band (better signal/noise ratio), in concentric annuli around emission peak
- Spectra are extracted in the 0.6-10keV band, and fitted with single temperature MEKAL model



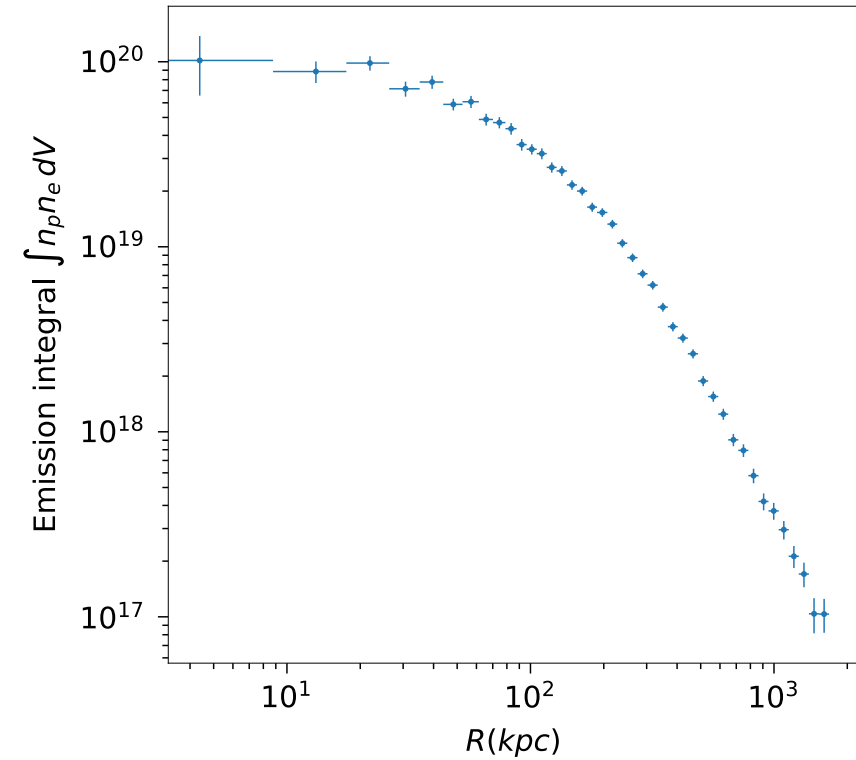
Typical source subtraction, point sources are in yellow and extended source in red

Analysis of X-ray data

Example of obtained profiles



Profile of Abell 2204, $z=0.164$, high data quality



Profile of Abell 2552, $z=0.300$, low data quality

Analysis of X-ray data

Calculating masses from X-ray: Yx scaling relation

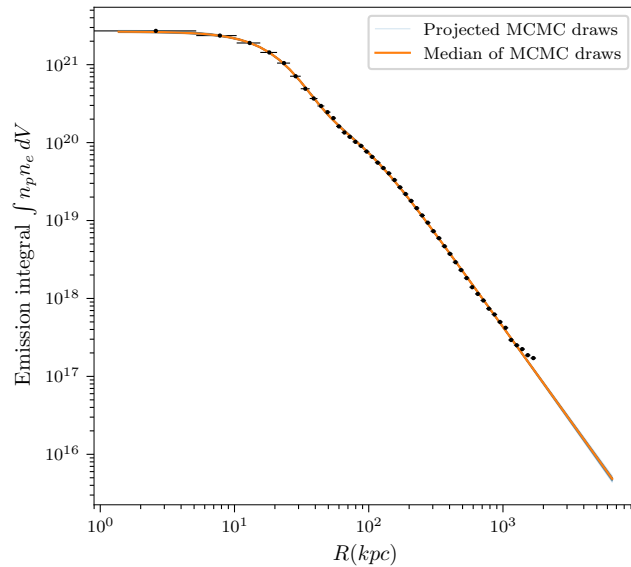
Use Vikhlinin et al. 2006 profile for density:

$$n_p n_e = n_0^2 \frac{(r/r_c)^{-\alpha}}{(1 + r^2/r_c^2)^{3\beta - \alpha/2}} \frac{1}{(1 + r^\gamma/r_s^\gamma)^{\varepsilon/\gamma}} + \frac{n_{02}^2}{(1 + r^2/r_{c2}^2)^{3\beta_2}}$$

Project 3D profiles to compare to 2D observations

Calculate masses using Vikhlinin et al. 2009 Yx-M500 scaling relation:

Iterative process since Yx is measured within R500:



Fitted profile of Abell 2204

Analysis of X-ray data

Calculating masses from X-ray: Yx scaling relation

Use Vikhlinin et al. 2006 profile for density:

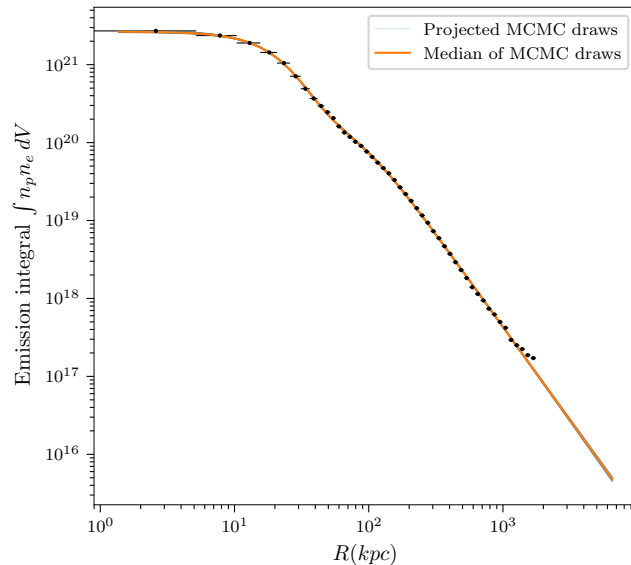
$$n_p n_e = n_0^2 \frac{(r/r_c)^{-\alpha}}{(1 + r^2/r_c^2)^{3\beta - \alpha/2}} \frac{1}{(1 + r^\gamma/r_s^\gamma)^{\varepsilon/\gamma}} + \frac{n_{02}^2}{(1 + r^2/r_{c2}^2)^{3\beta_2}}$$

Project 3D profiles to compare to 2D observations

Calculate masses using Vikhlinin et al. 2009 Yx-M500 scaling relation:

Iterative process since Yx is measured within R500:

1) First R500 value from T-M500 scaling relation (Vikhlinin et al. 2009)



Fitted profile of Abell 2204

Analysis of X-ray data

Calculating masses from X-ray: Yx scaling relation

Use Vikhlinin et al. 2006 profile for density:

$$n_p n_e = n_0^2 \frac{(r/r_c)^{-\alpha}}{(1 + r^2/r_c^2)^{3\beta-\alpha/2}} \frac{1}{(1 + r^\gamma/r_s^\gamma)^{\varepsilon/\gamma}} + \frac{n_{02}^2}{(1 + r^2/r_{c2}^2)^{3\beta_2}}$$

Project 3D profiles to compare to 2D observations

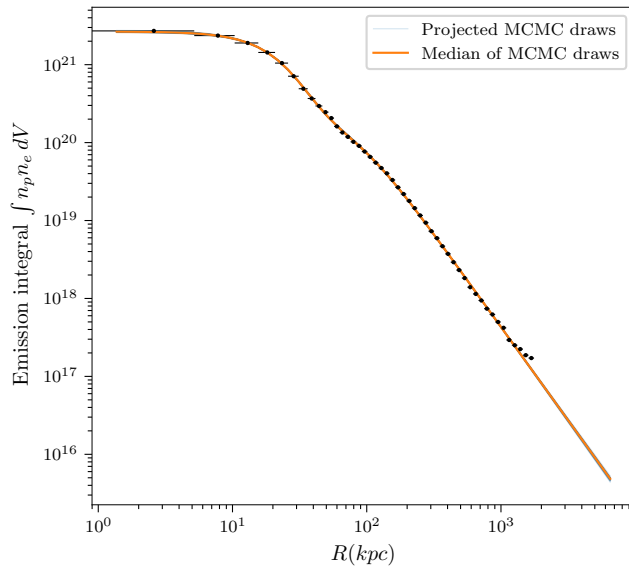
Calculate masses using Vikhlinin et al. 2009 Yx-M500 scaling relation:

Iterative process since Yx is measured within R500:

1) First R500 value from T-M500 scaling relation (Vikhlinin et al. 2009)

2) Measure core excised Tx in [0.15,1] R500, $Y_X = k T_{exc} M_{gas}^{500}$

3) Solve $\frac{4\pi}{3} 500 \rho_{crit}(z) R_{500}^3 = M_{500} = (5.77 \pm 0.20) \cdot 10^{14} h^{1/2} M_\odot \left(\frac{Y_X(R_{500})}{3 \cdot 10^{14} M_\odot \text{keV}} \right)^{0.57 \pm 0.03} E(z)^{-2/5}$
for R500 (Vikhlinin et al. 2009)



Fitted profile of Abell 2204

Analysis of X-ray data

Calculating masses from X-ray: Yx scaling relation

Use Vikhlinin et al. 2006 profile for density:

$$n_p n_e = n_0^2 \frac{(r/r_c)^{-\alpha}}{(1 + r^2/r_c^2)^{3\beta-\alpha/2}} \frac{1}{(1 + r^\gamma/r_s^\gamma)^{\varepsilon/\gamma}} + \frac{n_{02}^2}{(1 + r^2/r_{c2}^2)^{3\beta_2}}$$

Project 3D profiles to compare to 2D observations

Calculate masses using Vikhlinin et al. 2009 Yx-M500 scaling relation:

Iterative process since Yx is measured within R500:

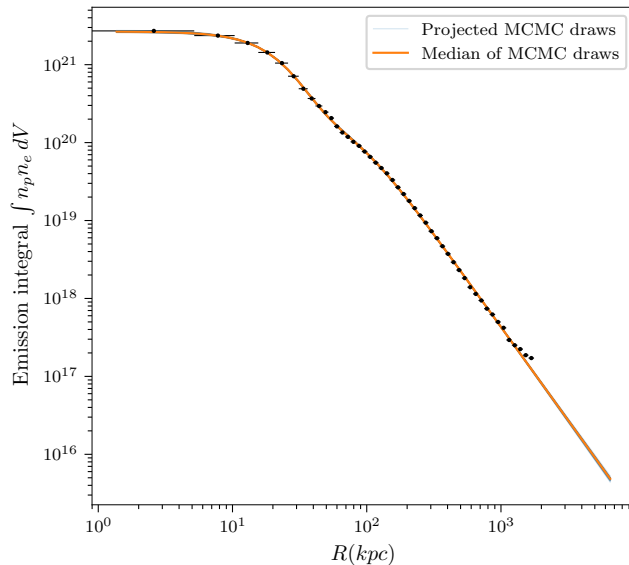
1) First R500 value from T-M500 scaling relation (Vikhlinin et al. 2009)

2) Measure core excised Tx in [0.15,1] R500, $Y_X = k T_{exc} M_{gas}^{500}$

3) Solve $\frac{4\pi}{3} 500 \rho_{crit}(z) R_{500}^3 = M_{500} = (5.77 \pm 0.20) \cdot 10^{14} h^{1/2} M_\odot \left(\frac{Y_X(R_{500})}{3 \cdot 10^{14} M_\odot \text{keV}} \right)^{0.57 \pm 0.03} E(z)^{-2/5}$
for R500 (Vikhlinin et al. 2009)

4) Iterate 2)&3)

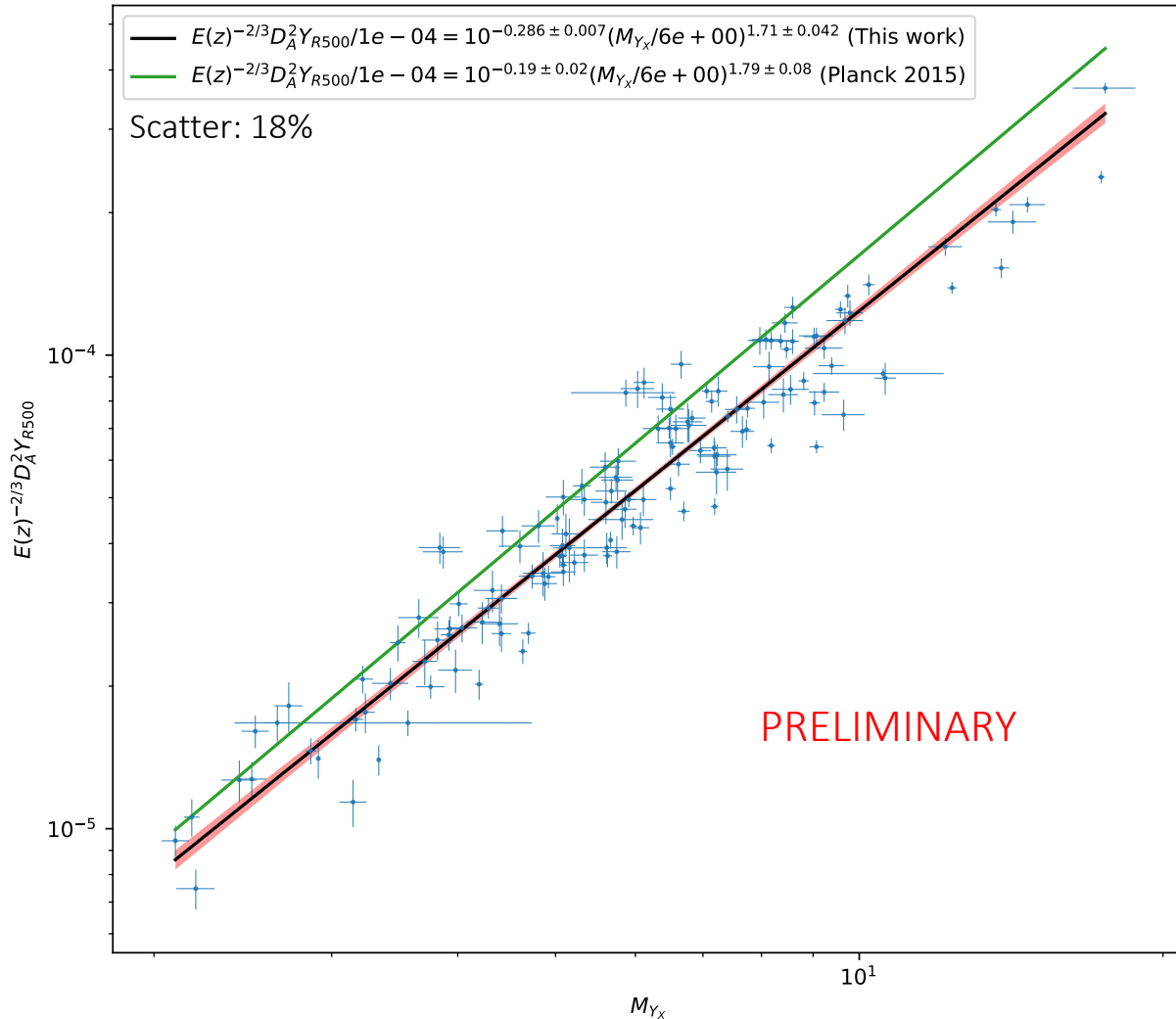
5) $M_{500} = (5.77 \pm 0.20) \cdot 10^{14} h^{1/2} M_\odot \left(\frac{Y_X(R_{500})}{3 \cdot 10^{14} M_\odot \text{keV}} \right)^{0.57 \pm 0.03} E(z)^{-2/5}$



Fitted profile of Abell 2204

Obtaining masses

Calibrating the Ysz-M relation



Run MMF algorithm with X-ray positions and apertures
Obtain Ysz with uncertainties

Correct for Malmquist bias:

Divide each individual Ysz by mean bias at that value

After adding statistical uncertainty and scatter from X-ray scaling relation:

$$E^{-2/3}(z) \frac{D_A^2 Y_{500}}{10^{-4} \text{Mpc}^2} = 10^{-0.29 \pm 0.01} \left(\frac{(1-b) M_{500}}{6 \cdot 10^{14} M_{\odot}} \right)^{1.71 \pm 0.1}$$

Scatter: 20%

Robust to choice of MCMC sampler (emcee, LinMix, BCES)

Obtaining masses

Comparison with Planck 2015 results

Preliminary scaling relation:

$$E^{-2/3}(z) \frac{D_A^2 Y_{500}}{10^{-4} \text{Mpc}^2} = \underline{10^{-0.29 \pm 0.01}} \left(\frac{(1-b) M_{500}}{6 \cdot 10^{14} M_\odot} \right)^{\underline{1.71 \pm 0.1}} \quad \text{Scatter: 20\%}$$

Planck collab. 2015 Cosmology from SZ number counts scaling relation :

$$E^{-2/3}(z) \left[\frac{D_A^2 Y_{500}}{10^{-4} \text{Mpc}^2} \right] = \underline{10^{-0.19 \pm 0.02}} \left(\frac{(1-b) M_{500}}{6 \times 10^{14} M_\odot} \right)^{\underline{1.79 \pm 0.08}} \quad \text{Scatter: 18\%}$$

The new scaling relation has:

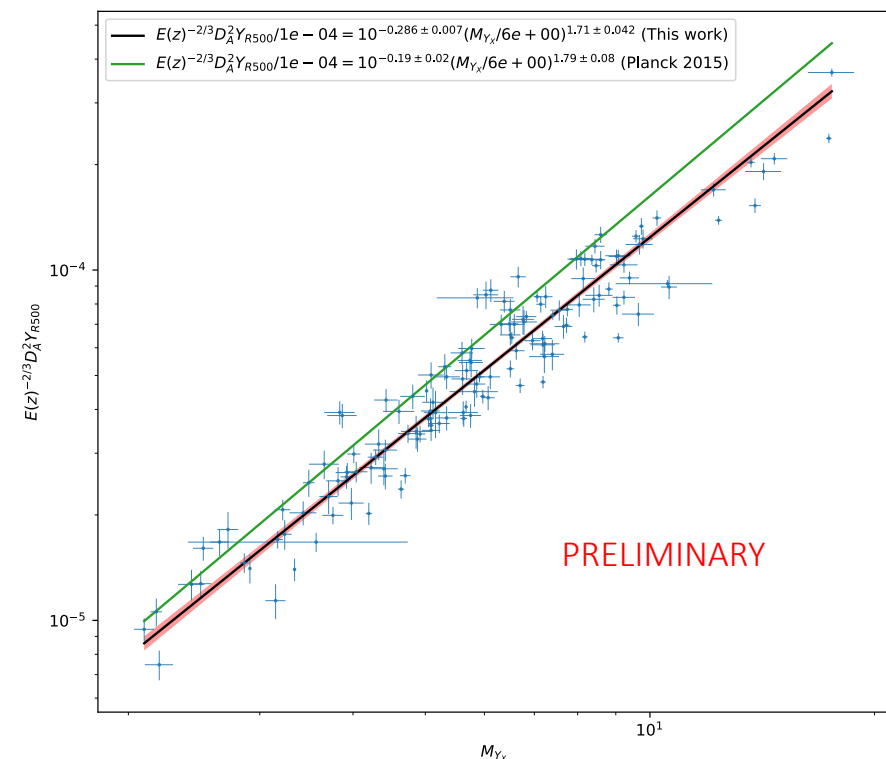
Lower normalization: Chandra and XMM temperature calibration don't match, Chandra measures hotter and thus heavier cluster. The **difference is coherent with predictions from Schellenberger et al. 2015** (20% difference)

Shallower slope: The new scaling relation is closer to self-similar (slope of 5/3)

Comparable uncertainties: Lower uncertainties on $Y_{SZ}-M_{Y_X}$ (larger sample) but higher uncertainties on $Y_X-M_{Y_X}$ compensates the difference

Constraining the cosmology

What are the effect of changing the scaling relation ?



Explore the influence of scaling relation parameters with **toy models**

Start from **Planck 2015 scaling relation** and free one parameter of scaling relation at a time

Rest of the analysis is identical to Planck 2015 Cosmology with SZ number counts:
Use **cosmology cluster sample**, **two dimensional likelihood** (fit number counts as function of redshift and S/R), **CCCP prior on mass bias**

$$\frac{dN}{dzdq} = \int d\Omega_{\text{mask}} \int dM_{500} \frac{dN}{dzdM_{500}d\Omega} P[q|\bar{q}_m(M_{500}, z, l, b)] \quad \text{Fitted number counts}$$

$$\frac{dN}{dzdM_{500}d\Omega} = \frac{dN}{dVdM_{500}} \frac{dV}{dzd\Omega} \quad \text{Theoretical mass function}$$

$$\bar{q}_m \equiv \bar{Y}_{500}(M_{500}, z) / \sigma_f[\bar{\theta}_{500}(M_{500}, z), l, b] \quad \text{Median S/R for given M and z}$$

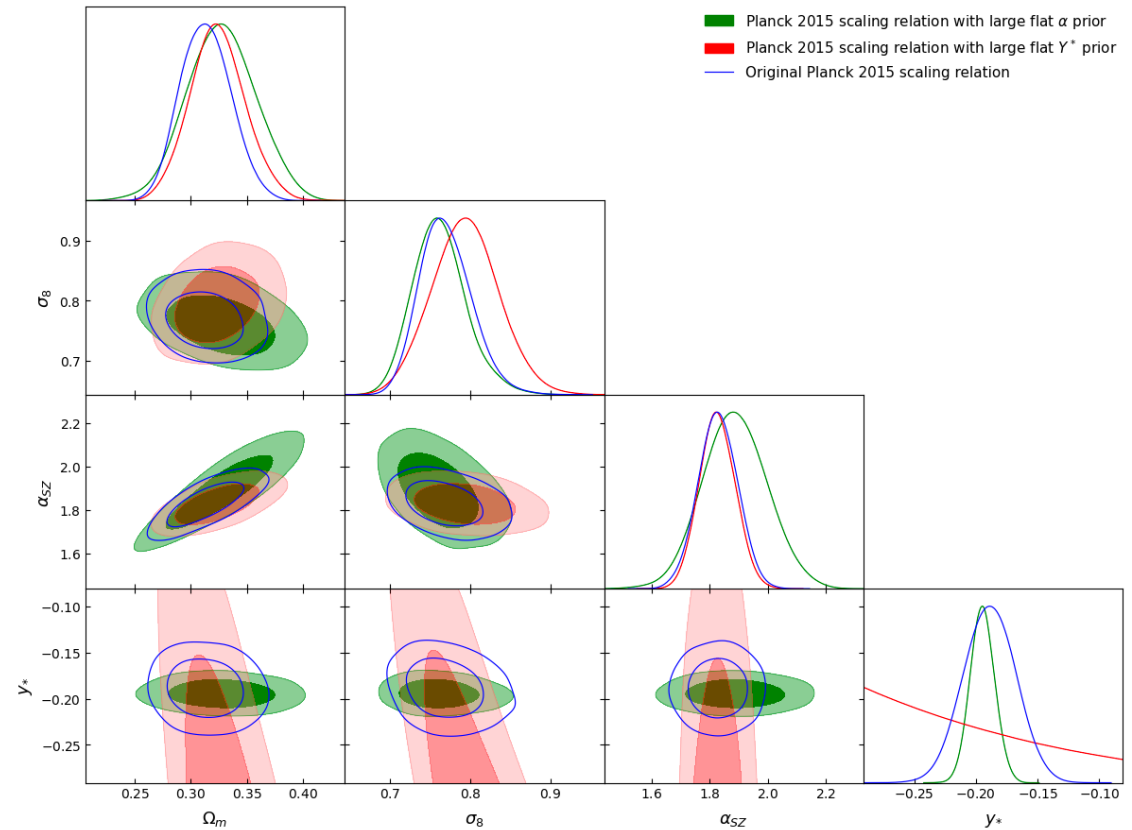
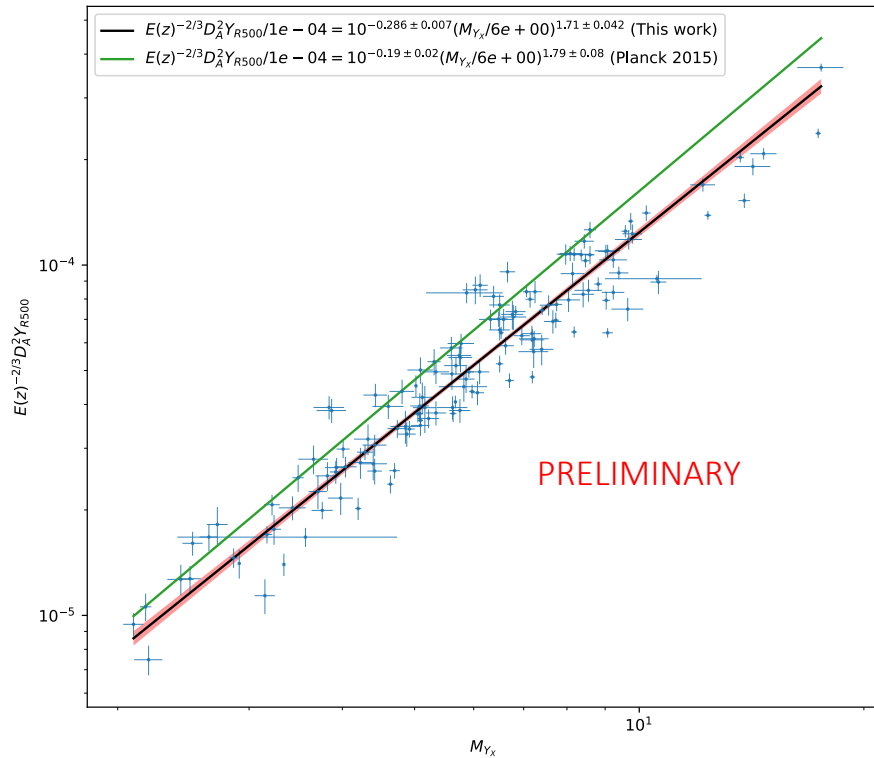
Scaling relation

Constraining the cosmology

What are the effect of changing the scaling relation ?

Lower normalisation: heavier clusters, higher σ_8

Change of slope: modifies ratio of high to low mass clusters, moves constraints along σ_8 - Ω_m degeneracy



Constraining the cosmology

Next step: internal calibration

$$E^{-2/3}(z) \frac{D_A^2 Y_{500}}{10^{-4} \text{Mpc}^2} = 10^{-0.29 \pm 0.01} \left(\frac{(1-b) M_{500}}{6 \cdot 10^{14} M_\odot} \right)^{1.71 \pm 0.1}$$



$$E^{-\beta}(z) \frac{D_A^2 Y_{500}}{10^{-4} \text{Mpc}^2} = Y_* \left(\frac{h}{0.7} \right)^{-2+\alpha} \left(\frac{(1-b) M_{500}}{6 \cdot 10^{14} M_\odot} \right)^\alpha$$

Include X-ray, SZ (and lensing data ?) in the likelihood and fit cosmological parameters and α , β , Y_* and b together



Obtain cosmological constraints from clusters using multi-wavelength information and marginalising over systematics

Other possible improvements: Use PR4 maps for SZ detections, explore other (lower uncertainty) mass estimates...

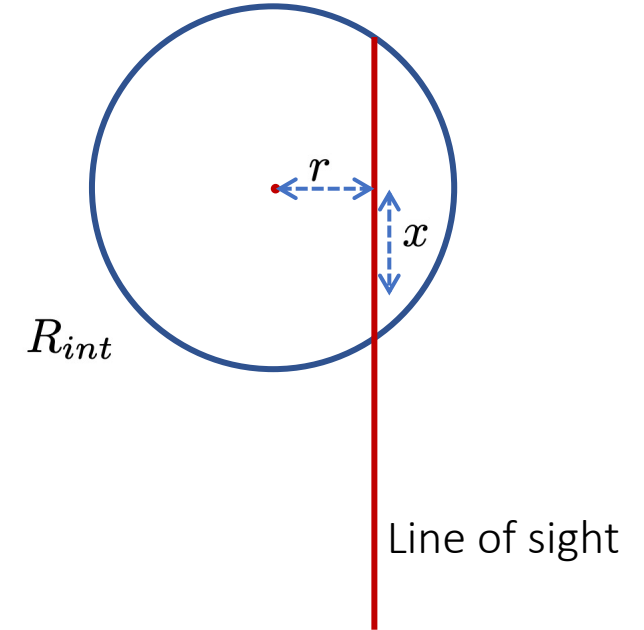
Appendix

Dealing with projection effects

The functions are made to fit 3D profiles, but observations are 2D projections along the line of sight
During fitting, 3D profiles are first projected then compared to 2D observations

In the case of density/emission integral we can neglect the bin width:

$$EI_i = 2 \int_0^{\sqrt{R_{int}^2 - r_i^2}} n_p n_e(\sqrt{x^2 + r_i^2}) dx \quad \text{where } R_{int} = 50R_{500}$$



In the case of temperature, we need to weight by density, account for a dependence on temperature (Mazzotta et al. 2004), and take bin width into account:

$$T_i = \frac{\int_{r_i}^{r_{i+1}} \int_1^{\sqrt{(R_{int})^2 - r^2}} r w T_{\text{fit}}(\sqrt{r^2 + x^2}) dx dr}{\int_{r_i}^{r_{i+1}} \int_1^{\sqrt{(R_{int})^2 - r^2}} r w dx dr} \quad \text{where } w = n_p n_e(\sqrt{r^2 + x^2}) T_{\text{fit}}^{-0.75}(\sqrt{r^2 + x^2}) \text{ and } R_{int} = R_{200}$$

Appendix

Masses from X-ray data

With X-ray data, we can compute masses under hydrostatic equilibrium assumption:

$$M_{HE}(< r) = -\frac{rk_B T(r)}{G\mu m_p} \left(\frac{d \ln \rho(r)}{d \ln r} + \frac{d \ln T(r)}{d \ln r} \right)$$

But clusters' dynamical states vary widely and the assumption can be quite false

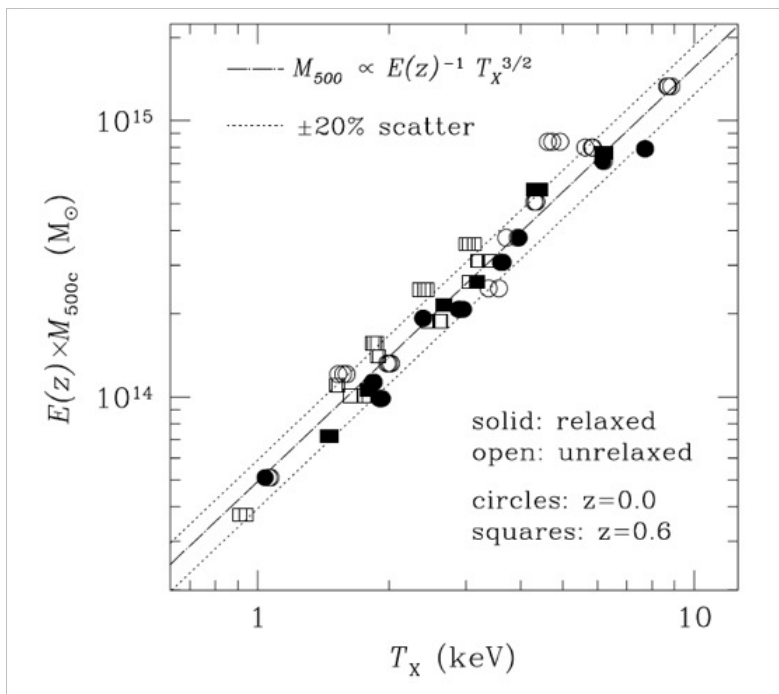
Instead of using the hydrostatic masses, scaling relations are commonly used:

- Calibrate relation between observable/hydrostatic mass for a set of relaxed clusters
- Use the relation to calculate other cluster masses

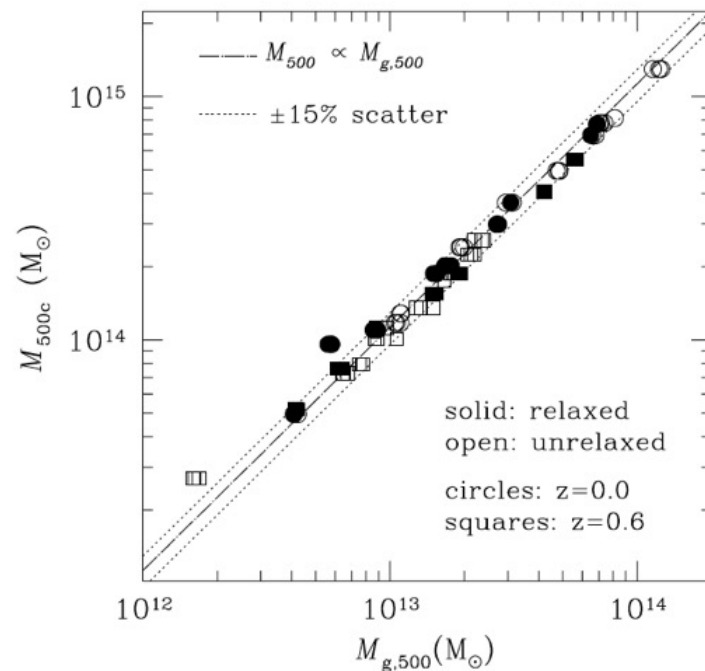
Appendix

What is the best proxy for mass ?

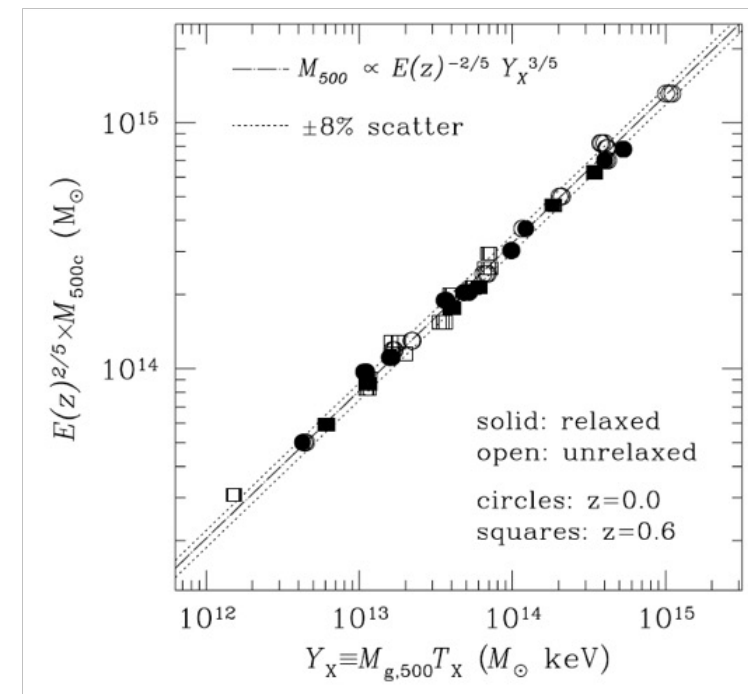
Kravtsov et al. 2006: comparison of proxies/true mass on simulated Chandra observations of clusters



20% scatter due to unrelaxed
 clusters mostly
 Unrelaxed cluster have lower T_x :
 Kinetic energy not fully converted
 to thermal during mergers
 Slope=self similarity



15% scatter
 Slope!=self similarity (0.92 ± 0.02)
 Due to f_{gas} varying with M & z



8% scatter
 No relaxed/unrelaxed distinction
 Less sensitive to departure from
 spherical symmetry
 Slope=self similarity

Y_x is a robust and self-similar proxy to mass

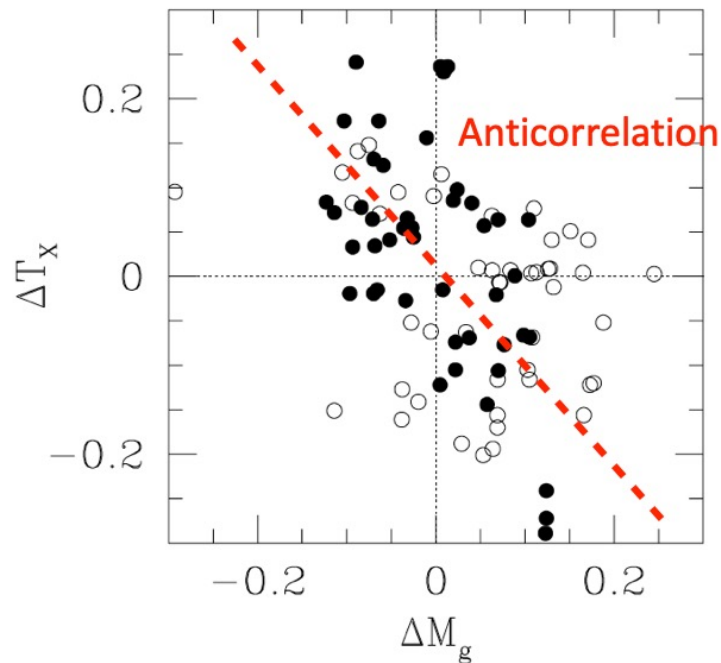


FIG. 5.—Fractional deviations in temperature and gas mass for fixed M_{500} relative to their respective best-fit self-similar relations, $M_{500} \propto T_X^{1.5}$ and $M_{500} \propto M_{g,500}$. The fit includes all systems, at both $z = 0$ (filled circles) and $z = 0.6$ (open circles). Note that the deviations for gas mass and temperature are generally anti-correlated: clusters with large positive (negative) deviations in $M_{g,500}$ tend to have negative (positive) deviations in T_X . A similar anticorrelation exists in the trend with redshift (compare the distribution of points for $z = 0$ and 0.6). [See the electronic edition of the Journal for a color version of this figure.]

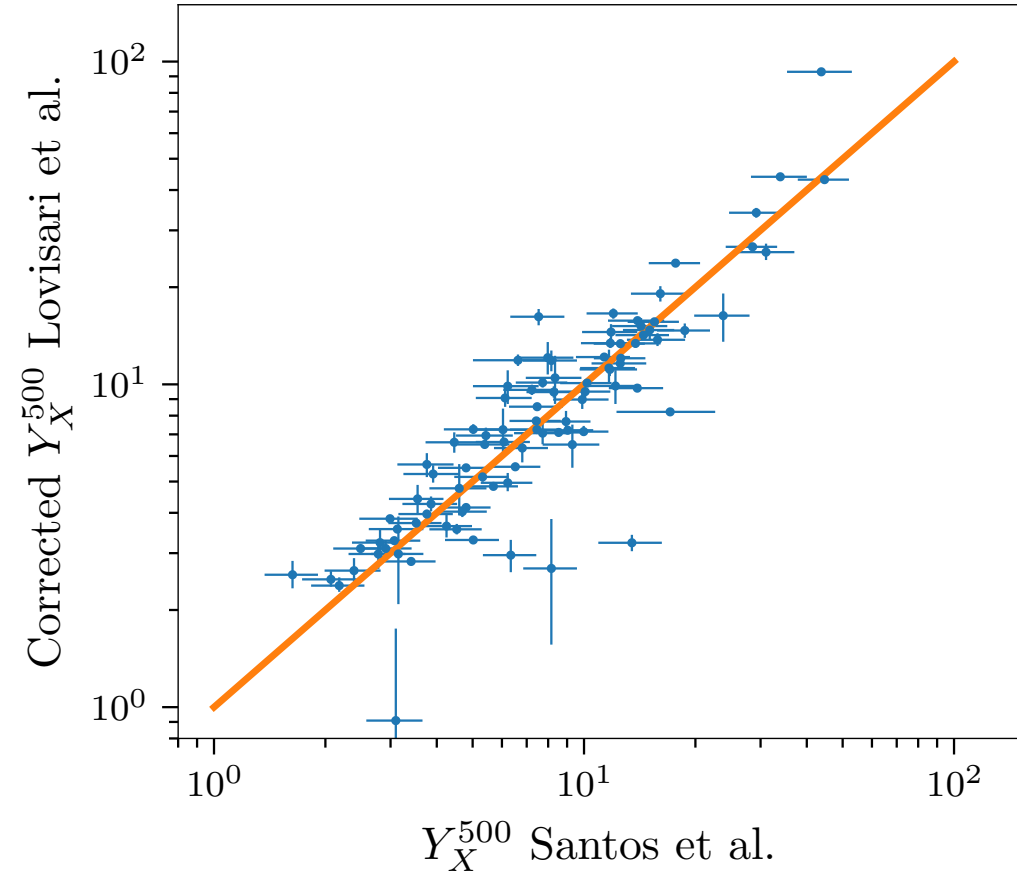
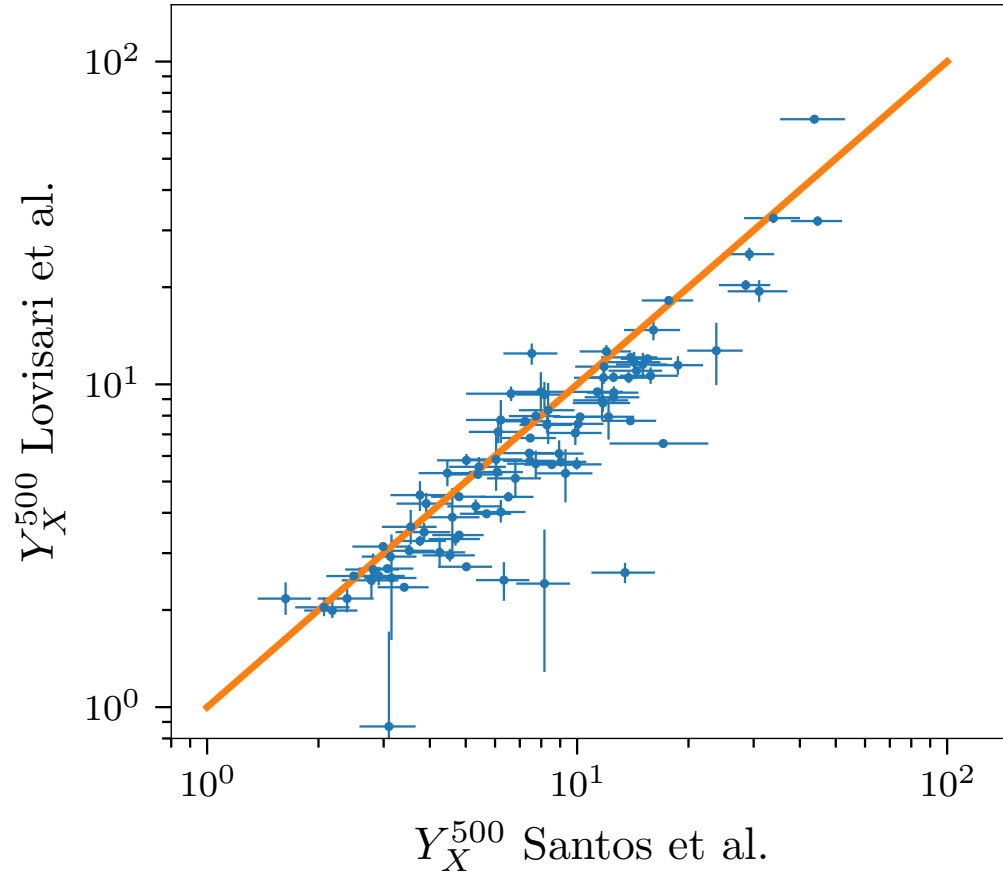
Why is Y_x a good proxy ?

Less relaxed clusters, over-estimation of M_g (non-uniform density, $\langle n^2 \rangle > \langle n \rangle^2$)
 Unrelaxed cluster have lower T_x : kinetic energy not fully converted to thermal during mergers

Appendix

XMM Newton vs Chandra

Temperature measurements don't match, leading to different Y_x values

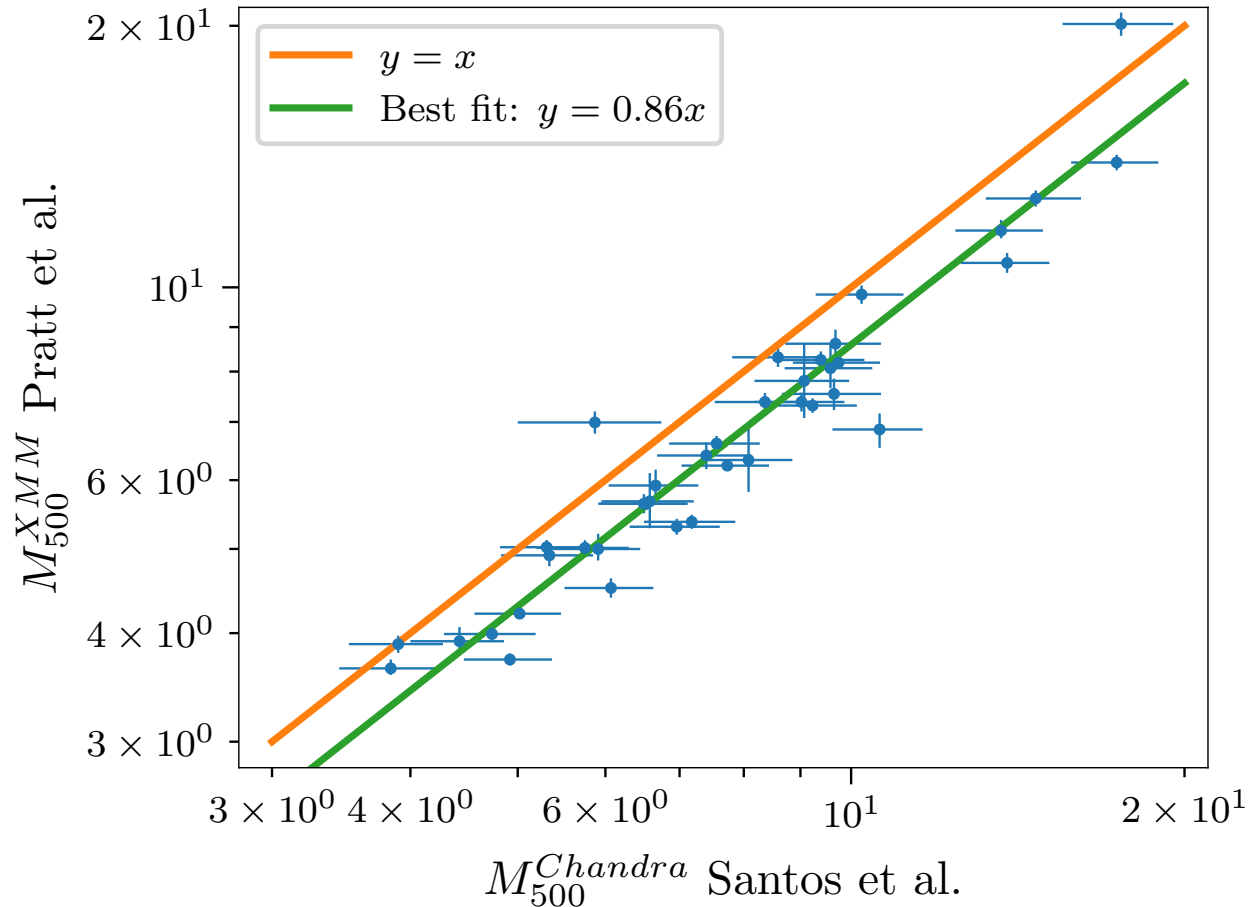


The temperature calibration can be accounted for, but the truth isn't known

Appendix

XMM Newton vs Chandra

Because the true temperature isn't known, and Y_x - M_{500} relations rely on HSE hypothesis, the masses inferred from Chandra and XMM differ



XMM scaling relation (Arnaud et al. 2010):

$$h(z)^{2/5} M_{500} = 10^{14.567 \pm 0.010} \left[\frac{Y_X}{2 \times 10^{14} h_{70}^{-5/2} M_{\odot} \text{ keV}} \right]^{0.561 \pm 0.018} h_{70}^{-1} M_{\odot}$$

Chandra scaling relation (Vikhlinin et al. 2009):

$$M_{500}^{Y_X} = E^{-2/5}(z) A_{YM} \left[\frac{Y_X}{3 \times 10^{14} M_{\odot} \text{ keV}} \right]^{B_{YM}}$$

$$A_{YM} = (5.77 \pm 0.20) \times 10^{14} h^{1/2} M_{\odot}$$

$$B_{YM} = 0.57 \pm 0.03$$

Schellenberger et al. 2015:

$$M_{500}^{XMM} = 0.859^{+0.017}_{-0.016} \cdot M_{500}^{Chandra})^{1.00 \pm 0.02}$$

The masses obtained from Y_x with XMM are 14% lower on average

Appendix

Malmquist bias

When studying the relation between signal and another observable for a signal-to-noise limited sample, the intrinsic scatter in the relation will lead to preferential detection of objects biased high w.r.t. the mean in the low signal range

This needs to be accounted for when calibrating a scaling relation, by dividing each Y_{SZ} by the mean bias at the corresponding signal to noise ratio

$$Y_{SZ}^{corrected} = Y_{SZ}/b$$

$$\ln b = \frac{\exp(-x^2/2\sigma^2)}{\sqrt{\pi/2} \operatorname{erfc}(-x/\sqrt{2}\sigma)} \sigma$$

$$\text{where } x = -\log\left(\frac{(S/N)}{(S/N)_{cut}}\right) \text{ and } \sigma = \sqrt{\ln[((S/N) + 1)/(S/N)]^2 + (\ln 10 \sigma_{int})^2}$$

